Journal of Structural Biology 178 (2012) 290–299

Contents lists available at SciVerse ScienceDirect

Journal of Structural Biology

journal homepage: www.elsevier.com/locate/yjsbi

Structure, composition, and mechanical properties of shark teeth

Joachim Enax [a], Oleg Prymak [a], Dierk Raabe [b], Matthias Epple [a,*]

[a] Institute of Inorganic Chemistry and Center for Nanointegration Duisburg-Essen (CeNIDE), University of Duisburg-Essen, Universitaetsstr. 5–7, 45117 Essen, Germany
[b] Microstructure Physics and Alloy Design, Max-Planck-Institut für Eisenforschung, Max-Planck-Str. 1, 40237 Düsseldorf, Germany

ARTICLE INFO

Article history:
Received 22 December 2011
Received in revised form 18 March 2012
Accepted 21 March 2012
Available online 5 April 2012

Keywords:
Biomineralization
Teeth
Calcium phosphate
Mechanical properties
Nanoindentation
Sharks

ABSTRACT

The teeth of two different shark species (*Isurus oxyrinchus* and *Galeocerdo cuvier*) and a geological fluoroapatite single crystal were structurally and chemically characterized. In contrast to dentin, enameloid showed sharp diffraction peaks which indicated a high crystallinity of the enameloid. The lattice parameters of enameloid were close to those of the geological fluoroapatite single crystal. The inorganic part of shark teeth consisted of fluoroapatite with a fluoride content in the enameloid of 3.1 wt.%, i.e., close to the fluoride content of the geological fluoroapatite single crystal (3.64 wt.%). Scanning electron micrographs showed that the crystals in enameloid were highly ordered with a special topological orientation (perpendicular towards the outside surface and parallel towards the center). By thermogravimetry, water, organic matrix, and biomineral in dentin and enameloid of both shark species were determined. Dentin had a higher content of water, organic matrix, and carbonate than enameloid but contained less fluoride. Nanoindentation and Vicker's microhardness tests showed that the enameloid of the shark teeth was approximately six times harder than the dentin. The hardness of shark teeth and human teeth was comparable, both for dentin and enamel/enameloid. In contrast, the geological fluoroapatite single crystal was much harder than both kinds of teeth due to the absence of an organic matrix. In summary, the different biological functions of the shark teeth ("tearing" for *Isurus* and "cutting" for *Galeocerdo*) are controlled by the different geometry and not by the chemical or crystallographic composition.

1. Introduction

Teeth represent the most highly mineralized and hardest tissues in mammals including humans (Dorozhkin and Epple, 2002; LeGeros, 1981; Lowenstam and Weiner, 1989; Mann, 2001). Their extraordinary mechanical properties are due to a special hierarchical arrangement of the constituent carbonated calcium-deficient hydroxyapatite ("bioapatite") crystals (Al-Sawalmih et al., 2008; Dunlop and Fratzl, 2010; Fabritius et al., 2009; Wang and Weiner, 1998a,b; Weiner and Addadi, 1997). For details on the structure of human teeth, see, e.g., Fincham et al. (1999) and Teaford et al. (2000). The compact outer part of human teeth is formed by enamel, consisting of μm-sized rods of apatite in a special arrangement with a low content of organic matrix (about 1 wt.%). Note that in amphibians and fish (e.g., sharks), the outer part of teeth is denoted as enameloid, whereas in mammals and reptiles it is denoted as enamel (Herold et al., 1980; Kemp, 1984). The interior of teeth consists of dentin, a bone-like phase of apatite nanocrystals and about 20 wt.% of organic matrix (mainly collagen) (LeGeros, 1981). Dentin is a porous structure with μm-sized dentin tubuli (Marten et al., 2010; Zabler et al., 2007). As in mammalian teeth, the structural building elements in shark teeth occur in a highly ordered hierarchical way (Lowenstam and Weiner, 1989). On the outside, hard and mineral-rich enameloid is present; on the inside, softer and less mineralized dentin.

In contrast to mammalian teeth, the shark teeth contain fluoroapatite, $Ca_5(PO_4)F$, as biomineral phase with partial substitutions of phosphate by carbonate and of fluoride by hydroxide (Daculsi and Kerebel, 1980; Moeller et al., 1975). Fluoroapatite has different mechanical properties than hydroxyapatite: it has a higher bulk modulus than hydroxyapatite (Brunet et al., 1999), higher stiffness constants and higher elastic moduli (Gardner et al., 1992), i.e., it is harder than hydroxyapatite. In teeth, the incorporation of fluoride ions into the apatite lattice protects the tooth against acids (LeGeros, 1990). Suga et al. (1982) showed in a comprehensive study that the teeth of many fish species contain fluoride, and that this is not related to feeding behavior or the fluoride content of the water.

Studies combining different analytical methods were reported on shark teeth, sometimes on fossilized shark teeth (Daculsi and Kerebel, 1980; Dahm and Risnes, 1999; Frazzetta, 1988; Gillis and Donoghue, 2007; Glas, 1962; Kesmez et al., 2004; LeGeros and Suga, 1980; Moeller et al., 1975; Powlik, 1995; Preuschoft et al., 1974; Reif, 1974; Whitenack and Motta, 2010; Whitenack et al., 2011, 2010). Here we report on a comprehensive study of

* Corresponding author. Fax: +49 (0) 201 183 2621.
E-mail address: matthias.epple@uni-due.de (M. Epple).

1047-8477/$ - see front matter © 2012 Elsevier Inc. All rights reserved.
http://dx.doi.org/10.1016/j.jsb.2012.03.012

the chemical composition, the (ultra)structure, and the micromechanical properties, separately for dentin and enameloid, of two shark species (*Isurus oxyrinchus*, shortfin mako shark; and *Galeocerdo cuvier*, tiger shark). This permits the correlation of all parameters, specifically between structure and hardness. We have chosen teeth of these two species because the teeth have different functions and thus it was possible to correlate function with structure and hardness. The shape of the teeth of *I. oxyrinchus* and *G. cuvier* and their function are different. Teeth of *I. oxyrinchus* are interior curved and are used to rupture the prey. Teeth of *G. cuvier*, on the other hand, have serrated margins and are mainly used for cutting the prey like a "saw". Thus teeth of *I. oxyrinchus* were denoted as "tearing" teeth and teeth of *G. cuvier* were denoted as "cutting" teeth by Whitenack and Motta (2010).

The fact that shark teeth consist of the harder biomaterial fluoroapatite may have implications for their biological function, especially in comparison to mammalian and human teeth. To elucidate the relationship between chemical composition, biomaterial structure and mechanical properties was the aim of this work. As complementary sample, a human wisdom tooth was mechanically analyzed under identical measuring conditions. For a comparison with the pure mineral (i.e., without any organic matrix), a geological fluoroapatite single crystal was analyzed as well.

2. Materials and methods

2.1. Sample preparation and analytical methods

Recent shark teeth of *I. oxyrinchus* and *G. cuvier* were obtained from an online store. The shark species were taxonomically determined with the help of Dr. A. Gillis, University of Cambridge. The teeth were delivered and stored in dry state at room temperature. For a comparison between shark teeth and human teeth, a human wisdom tooth was mechanically characterized as well. The human wisdom tooth was caries-free and was explanted because of medical reasons. As reference material, a geological fluoroapatite single crystal was analyzed. Its identity was confirmed by X-ray powder diffraction. Crystalline hydroxyapatite as reference material was obtained from Sigma–Aldrich in p.a. quality (reagent grade, synthetic white powder; IR spectrum, X-ray powder diffractogram, calcium content, and phosphate content corresponded to this specification).

Infrared (IR) spectroscopy and X-ray powder diffraction (XRD) measurements were used to identify chemical compounds, to analyze the differences in the crystallinity of dentin and enameloid and to determine the crystallite size. For IR spectroscopy and XRD measurements, the shark teeth were transversally cut with a Proxxon fine drill and polishing tool FBS 230/E, equipped with a diamond-coated cutting disk and a diamond-coated drill. A fine powder of enameloid and dentin (a few mg per sample) was obtained with the same instrument from the corresponding areas of the cut teeth. The geological fluoroapatite single crystal was mechanically abraded in the same way to a fine powder which was then used for elemental analysis, X-ray diffraction, and IR spectroscopy. Fourier-transform infrared spectroscopy (FTIR) was carried out with a Bruker Vertex 70 instrument in KBr pellets (range 400–4000 and 2 cm^{-1} resolution). X-ray powder diffraction was carried out with a Bruker D8 Advance diffractometer (Cu K_α radiation, λ = 1.54 Å), using a silicon single crystal as sample holder to minimize scattering. Rietveld refinement for the calculation of the lattice parameters and the crystallite sizes was performed with the Bruker software TOPAS 4.2. For each Rietveld refinement the instrumental correction was included as determined with a standard powder sample LaB_6 (from NIST, National Institute of Standards and Technology, as standard reference material, SRM 660b). The size of the crystallites was calculated with the Scherrer equation after correction for instrumental peak broadening (Klug and Alexander, 1974).

Elemental analysis was carried out to determine the overall chemical composition of the samples and to confirm the identity of the mineral phases. For the determination of calcium, magnesium and sodium with atomic absorption spectroscopy (AAS), fluoride with ion-selective potentiometry, and phosphate with ultraviolet (UV) spectroscopy, about 100 mg powder of dentin and enameloid were used after dissolution in hydrochloric acid. For fluoride analysis we used ion-selective potentiometry (ion-selective electrode, ISE; pH/ION 735, WTW; measurement performed by Analytische Laboratorien GmbH, Lindlar, Germany). Calcium, sodium, and magnesium were determined with a Thermo Electron, M-Series atomic absorption spectrometer. Phosphate was analyzed with a Varian Cary 300 UV–Vis spectrophotometer as phosphate–molybdenum blue complex.

Thermogravimetry (TG) was used to determine the contents of water, organic matrix, and carbonated apatite in the teeth. For TG analysis, the teeth were transversally cut. To obtain almost pure enameloid, we cut off the tip of the tooth (about 70 mg per tooth) for analysis. To obtain almost pure dentin, we used the lower part of the tooth where it met the root (about 70 mg per tooth). Mechanical abrasion of enameloid and dentin was not performed for TG measurements to avoid a damage of the organic matrix by the high temperature caused by abrasion. Thermogravimetry was carried out with a Netzsch STA 449 F3 Jupiter instrument in dynamic oxygen atmosphere (heating rate 2 K min^{-1} from 25 to 1200 °C; open alumina crucibles).

Scanning electron microscopy (SEM) was used to visualize the internal structure of dentin, enameloid, and the dentin–enameloid junction. For transversal freeze fracture, the teeth were immersed into liquid nitrogen for 2 min and mechanically broken into two pieces. For SEM in backscattering electron mode (BSE) and indentation tests, the teeth were axially and transversally cut with a diamond saw and embedded in a phenolic resin with carbon fibers (Polyfast, Struers) with a heated press (150 bar, 5 min heating time, 180 °C; SimpliMet 3000 instrument, Buehler). The samples were ground with sandpaper with a grit size of 120, 220, 400, 600 and 1000 (Hermes), subsequently, and then polished first with a 3 μm diamond suspension (Struers), and finally with a 0.1 μm silica suspension (Buehler; Saphir 320/330 instrument, ATM). Secondary electron (SE) scanning electron microscopy (SEM) and energy-dispersive X-ray spectroscopy (EDX) were carried out with an ESEM Quanta 400 FEG instrument after sputtering with gold and palladium (80:20). SEM-BSE was carried out with a JEOL JSM-6500F instrument.

The mechanical properties of the samples were probed by micro- and nanoindentation on samples polished as described above. Nanoindentation measurements were conducted with a Hysitron TriboIndenter equipped with a Berkovich indenter (Ti 39–01, tip radius 50 nm). A constant load of 300 μN was applied (load control triangle 10–10 s). For representative results, 400 indentations in a 20 × 20 pattern (distance between the indentations 10.5 μm) were made for each chosen area at different positions in dentin and enamel(oid) of shark and human teeth and in the geological fluoroapatite single crystal. As reference, a fused quartz standard from Hysitron was used. The calculation of the reduced elastic modulus and the hardness was performed according to previous work (Oliver and Pharr, 1992; Sachs et al., 2006). Vicker's microhardness tests were carried out with a microhardness testing machine Leco M-400-H1. A weight of 10 g (HV0.01) was applied for 15 s, and eight indentations were made in the dentin or enamel(oid) of shark and human teeth, respectively. The experiments, including the distance between two indentations, was performed according to DIN EN ISO 6507-1 and DIN EN ISO 6507-4. The Vicker's hardness

HV0.01 was converted into nanohardness (Berkovich) *H* according to *HV0.01*/kg mm^{-2} = 92.65 s^2 m^{-1}·*H*/GPa.

Mechanical testing was performed on parts of the geological fluoroapatite single crystal that were embedded and polished in the same way as the teeth. Indentation was performed both on hexagonal faces (basal plane; indentations parallel to [001]) and side faces (prism plane; indentations perpendicular to [001]).

3. Results

Teeth of two different species were investigated with a geological fluoroapatite single crystal as reference material (Fig. 1). Scanning electron microscopy on axial cuts of the teeth clearly showed the interface between dentin and enameloid (Figs. 2 and 5). At the dentin–enameloid interface (dentin–enameloid junction), the fibers of the organic matrix were intertwined with the larger enameloid crystals, probably enhancing the adhesion between dentin and enameloid. The crystals in the enameloid of *I. oxyrinchus* were highly ordered with a special topological orientation which turned perpendicular towards the surface ("parallel-fibered layer"). The enameloid crystals met the surface, and a thin unstructured layer ("shiny layer enameloid") with a thickness of a few μm formed the outermost layer (Fig. 2). For the specific names of tissue layers in the enameloid see Gillis and Donoghue (2007). This shiny layer enameloid was also found in the teeth of *G. cuvier* (Fig. 5). Although the teeth differed in size (Fig. 1), the thickness of the shiny layer enameloid of both species was comparable.

A view on the transversal cross section of a tooth of *I. oxyrinchus* obtained by freeze-fracturing showed that the crystals were oriented perpendicular to each other, probably to provide a higher mechanical strength of the whole biocomposite (Al-Sawalmih et al., 2008). All crystal rods consisted of smaller fiber-like crystals as shown in the high resolution SEM images (Fig. 3). These crystalline rods had a diameter of a few μm and were not single crystals but rather fibrous crystal bundles. Similar bundles were also found in the enameloid of *G. cuvier* (not shown). Teeth of *Carcharhinus*

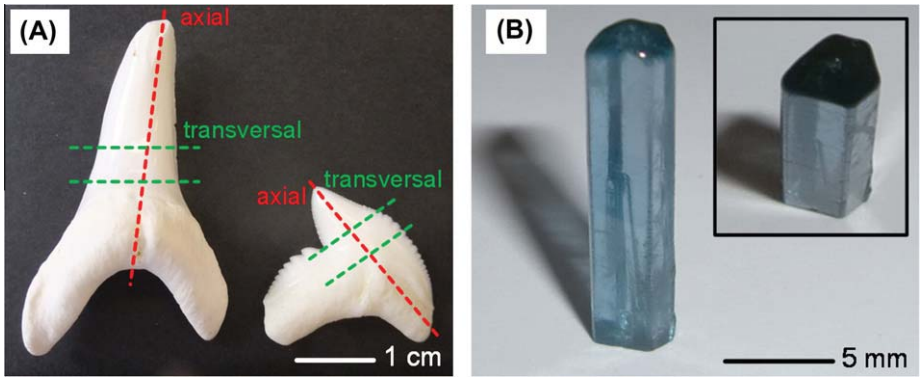

Fig.1. Images of the shark teeth used including the cutting planes (A; left: *Isurus oxyrinchus*; right: *Galeocerdo cuvier*) and an image of the geological fluoroapatite single crystal with an additional view on the top (B).

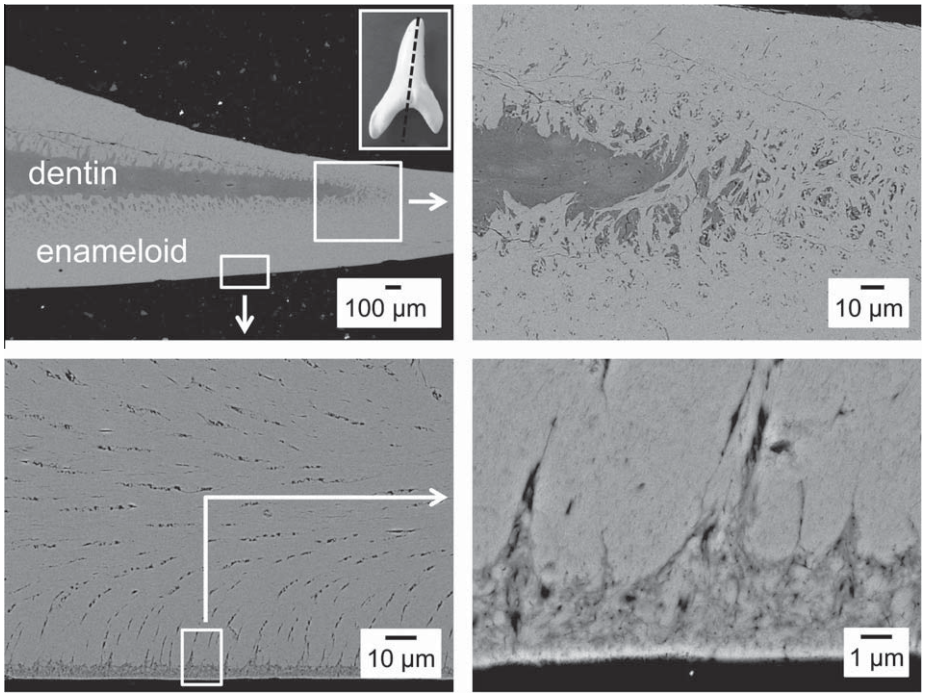

Fig.2. Scanning electron micrographs (back-scattered electron mode) of the axial cross section (see insert) of a tooth of *Isurus oxyrinchus*, showing the interface between dentin and enameloid (dentin–enameloid junction) and also the topological arrangement of the apatite crystals in the enameloid in different magnifications.

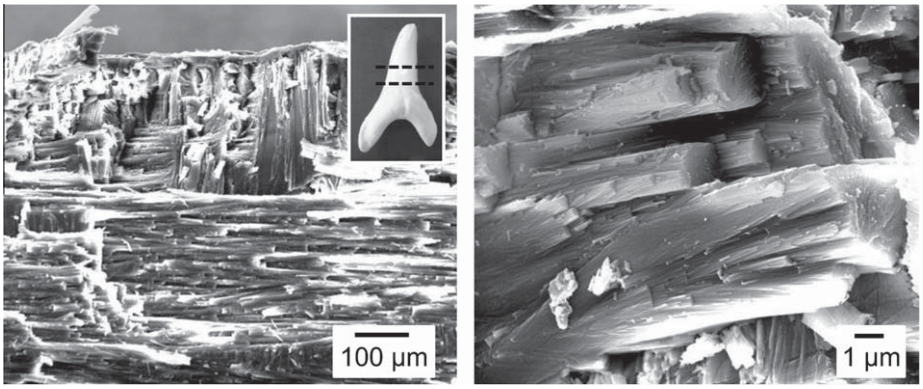

Fig.3. Scanning electron micrographs (secondary electron mode) of a transversal freeze-fractured surface (see insert) of the enameloid of a tooth of *Isurus oxyrinchus*.

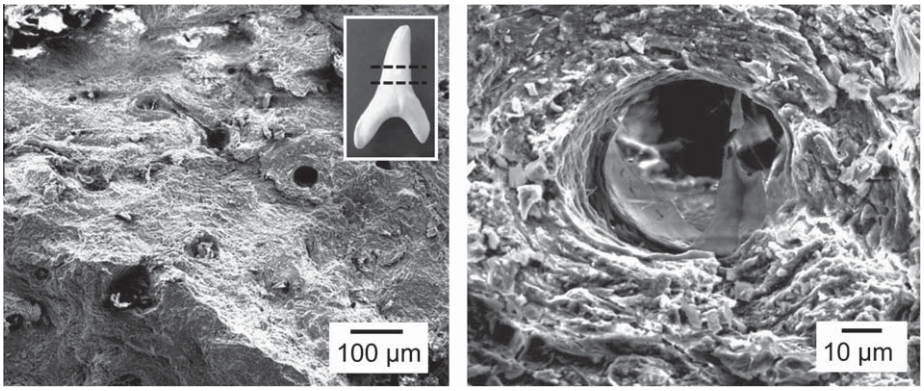

Fig.4. Scanning electron micrographs of a transversal freeze fracture surface (see insert) of the dentin of a tooth of *Isurus oxyrinchus* (secondary electron mode), showing the open dentin tubuli.

plumbeus show a similar enameloid microstructure, although the shiny layer enameloid was absent, in contrast to the shark teeth presented here (Gillis and Donoghue, 2007).

The dentin contained smaller inorganic crystals (invisible in the SEM, but detectable by XRD), an organic matrix and dentin tubuli as in human teeth (Stock et al., 2008; Zabler et al., 2007). Shark dentin tubuli were µm-sized as in human teeth (Absi et al., 1987; Kovtun et al., 2012; Zabler et al., 2007) (Figs. 4 and 6).

Mechanical tests were carried out at different positions of the teeth of both species (axial and transversal; enameloid and dentin) using nanoindentation (nanohardness) and Vicker's hardness tests (microhardness). In every area as indicated in Fig. 7, 400 indentations were made with reasonable reproducibility (Fig. 8). An overview of the areas for Vicker's indentation is shown in Fig. 9. The nanohardness of dentin (about 1 GPa) and enameloid (about 6 GPa) for *I. oxyrinchus* and *G. cuvier* teeth did not significantly differ (Tables 1 and 2). The same was found for the reduced elastic modulus of dentin (about 30 GPa) and enameloid (about 100 GPa).

Enameloid was about six times harder than dentin due to its higher mineral content. The differences in hardness between dentin and enameloid were also confirmed by different nanoindentation depths (ca. 70–130 nm for dentin and ca. 20–50 nm for enameloid).

The nanohardness was the same for axial and transversal cuts, which shows that the nanohardness of the shark teeth was isotropic within the experimental error limit. In the case of microhardness testing, a far larger area of the sample is subjected to mechanical indentation, therefore, the results from nanoindentation and microindentation are not strictly comparable. However, the trend of nanohardness was confirmed: the values for the two shark species were of the same magnitude and did not depend on axial or transversal direction. The geological fluoroapatite crystal was harder than the biological samples. No significant anisotropy of the hardness was found between basal faces and side faces in nanoindentation, but it was significant in microindentation. Notably, the cracks that formed on a side face after microindentation were larger than those on a hexagonal basal face, giving an explanation for the observed anisotropy (Fig. 10).

The quantification of the incorporation of fluoride in the apatite lattice and hence the presence of fluoroapatite in shark teeth by EDX was difficult because there were only small peaks of fluorine in the EDX-spectra. Fluorine is a light element and the X-ray yield is very low because the Auger effect dominates for light elements (Dyson, 2005). All elements which were found by EDX (except for C and O) were quantitatively determined with AAS (Ca^{2+}, Na^{+}, Mg^{2+}), UV-spectroscopy (PO_4^{3-}) and ion-selective potentiometry of fluoride (Table 3).

The apatite mineral in the teeth was identified by X-ray powder diffraction (Fig. 11). Fluoroapatite has a hexagonal structure with the space group $P6_3/m$ and the lattice parameters *a* and *c* (Rodriguez-Lorenzo et al., 2003). The lattice parameters *a* and *c* of the shark teeth are given in Table 4. The crystallite size (domaine size) is shown in Table 5.

The dentin and enameloid of both shark species showed a significant anisotropy in the crystallite size (Table 5). In *c*-direction, the crystallites were larger as indicated by the narrower diffraction peaks in (001) direction. Similar results were reported for bone samples by Peters et al. (2000). The crystallites of *I. oxyrinchus* were larger than of *G. cuvier*.

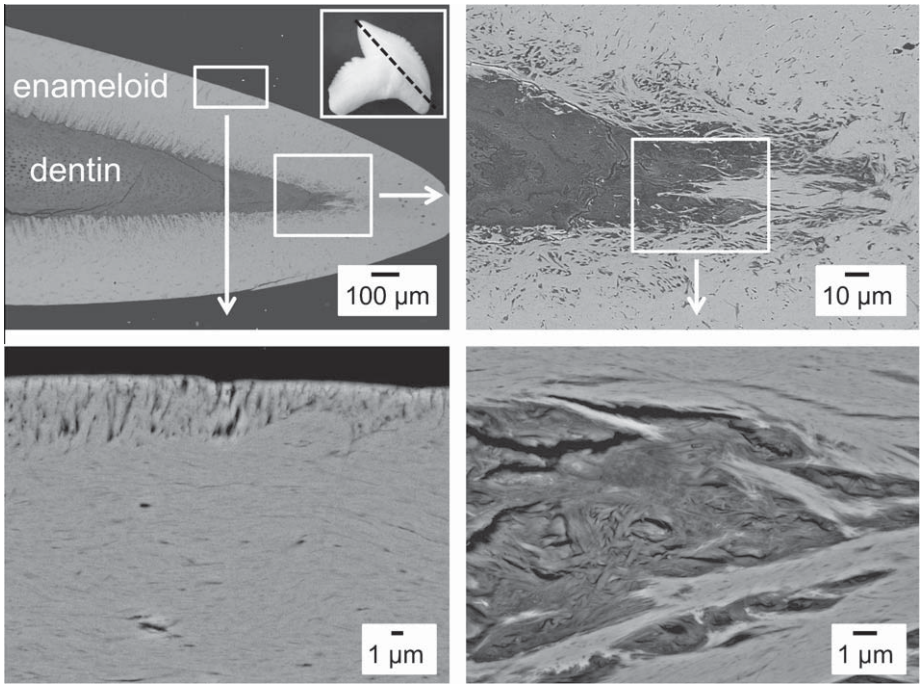

Fig.5. Scanning electron micrographs of an axial cross section-polished surface (see insert) of a tooth of *Galeocerdo cuvier*, showing the dentin–enameloid junction (back-scattered electron mode).

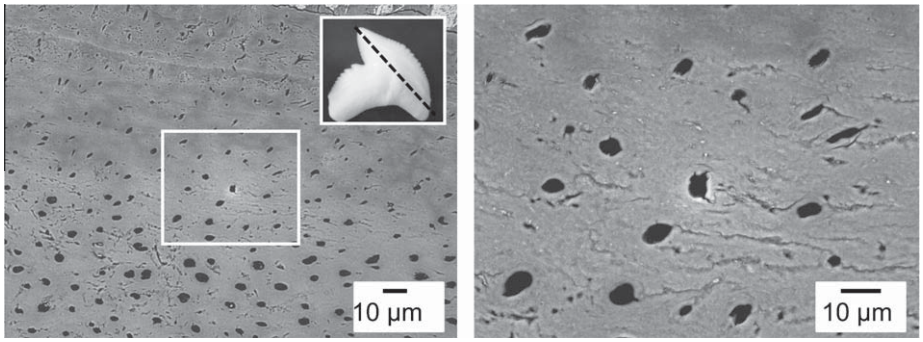

Fig.6. Scanning electron micrographs of an axial cross section-polished surface (see insert) of a tooth of *Galeocerdo cuvier*, showing the dentin tubuli (back-scattered electron mode).

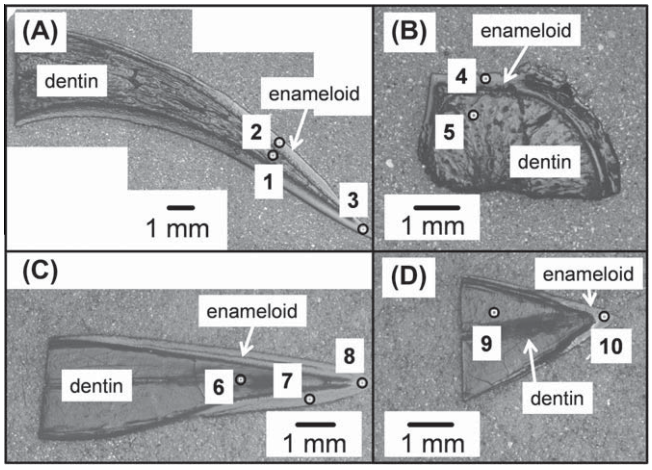

Fig.7. Nanoindentation on a cross section-polished surface of a tooth of *Isurus oxyrinchus* (A and B) and *Galeocerdo cuvier* (C and D), showing the numbered areas for 400 nanoindentations in each white square (highlighted by black circles) (A and C: axial cuts; (B and D) transversal cuts).

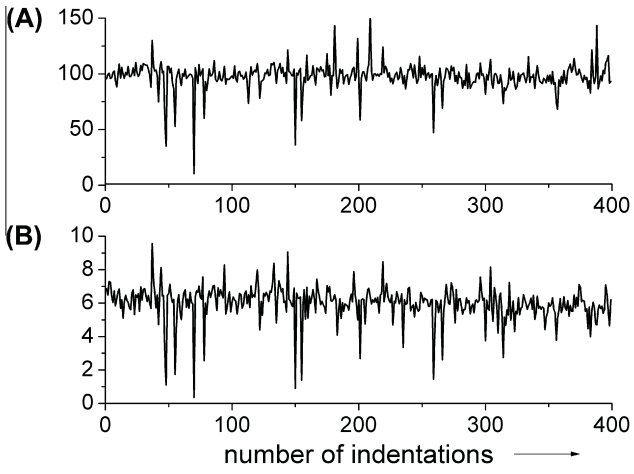

Fig.8. Representative results of 400 nanoindentations on a tooth of *Galeocerdo cuvier* (position 2 from Fig. 7, enameloid): reduced elastic modulus (A) and hardness (B) (both in GPa).

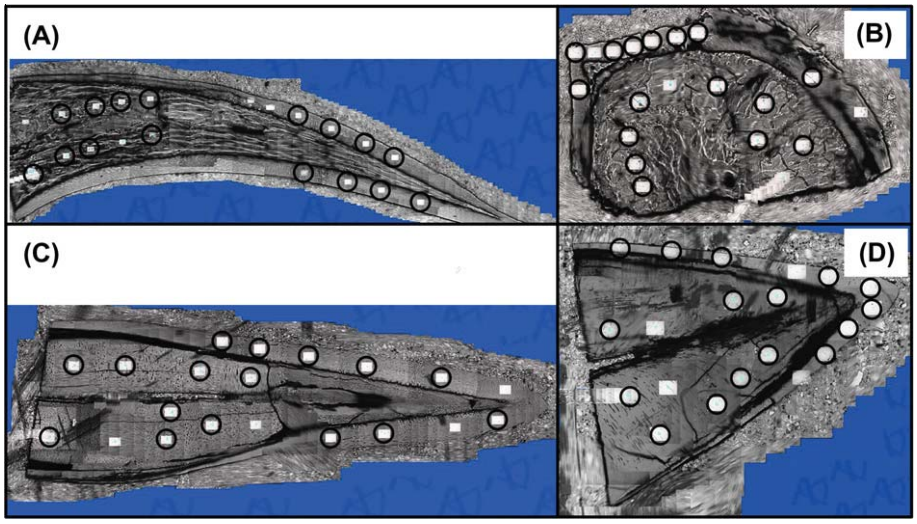

Fig.9. Vicker's indentation on a cross section-polished surface of a tooth of *Isurus oxyrinchus* (A and B) and *Galeocerdo cuvier* (C and D), showing the areas for eight Vicker's indentations (white squares for each indentation, highlighted by black circles) (A and C: axial cuts; B and D: transversal cuts).

Table 1
Results of nanoindentation of teeth of *Galeocerdo cuvier* and *Isurus oxyrinchus* (for positions **1**–**10** see Fig. 7), of a human tooth, and of a geological fluoroapatite single crystal. The average of 400 indentations ± standard deviation is given. The direction of the indentation was always perpendicular to the cut direction of the tooth. Hardness (H) and reduced elastic modulus (E_r) are both given in GPa.

Sample	Cut	Hardness (GPa)	Reduced elastic modulus (GPa)
Isurus oxyrinchus	1 (dentin, axial)	1.3 ± 0.4	32 ± 10
	2 (enameloid, axial)	6.2 ± 1.4	99 ± 17
	3 (enameloid, axial, tip)	7.5 ± 1.3	131 ± 19
	4 (dentin, transversal)	2.1 ± 0.4	49 ± 5
	5 (enameloid, transversal)	6.8 ± 0.9	127 ± 14
Galeocerdo cuvier	6 (dentin, axial)	0.7 ± 0.3	17 ± 5
	7 (enameloid, axial)	6.0 ± 1.0	98 ± 12
	8 (enameloid, axial, tip)	5.8 ± 1.0	94 ± 12
	9 (dentin, transversal)	1.2 ± 0.3	32 ± 6
	10 (enameloid, transversal)	6.1 ± 0.8	100 ± 11
Human tooth (this work)	Dentin, axial	1.4 ± 0.8	30 ± 8
	Enamel, axial	7.0 ± 0.6	109 ± 6
	Enamel, axial, tip	7.6 ± 0.5	116 ± 5
	Dentin, transversal	1.3 ± 0.6	30 ± 7
	Enamel, transversal	6.3 ± 0.8	106 ± 7
Human tooth (Marshall et al., 2001)	Dentin	1.0 ± 0.1	21 ± 2
Human tooth (Willems et al., 1993)	Enamel	3.4 ± 0.2	91 ± 16
Geological fluoroapatite single crystal (this work)	Basal faces	11.3 ± 0.8	148 ± 9
	Side faces	11.9 ± 0.8	153 ± 8
Geological hydroxyapatite single crystal (Saber-Samandari and Gross, 2009)	Basal faces	7.1	150.4
	Side faces	6.4	143.6
Synthetic hydroxyapatite whiskers (Viswanath et al., 2007)	Basal faces	9.7 ± 0.1	135.1 ± 1.3
	Side faces	8.8 ± 0.4	125.9 ± 1.6

Table 2
Results of Vicker's hardness tests (HV0.01; microhardness) of teeth of *Galeocerdo cuvier* and *Isurus oxyrinchus*, of a human tooth, and of a geological fluoroapatite single crystal. The average of eight indentations ± standard deviation is given. The direction of the indentation was always perpendicular to the cutting direction of the tooth (in kg mm^{-2}). In parentheses, the computed Berkovich-hardness (in GPa) is given.

Sample	Cut	Dentin	Enamel(oid)
Isurus oxyrinchus	Axial	34 ± 10 (0.4 ± 0.1)	284 ± 78 (3.1 ± 0.8)
	Transversal	52 ± 29 (0.6 ± 0.3)	301 ± 117 (3.2 ± 1.3)
Galeocerdo cuvier	Axial	36 ± 4 (0.4 ± 0.04)	368 ± 34 (4.0 ± 0.4)
	Transversal	38 ± 4 (0.4 ± 0.04)	343 ± 45 (3.7 ± 0.5)
Human tooth (this work)	Axial	58 ± 3 (0.6 ± 0.03)	385 ± 19 (4.2 ± 0.2)
	Transversal	66 ± 3 (0.7 ± 0.03)	401 ± 24 (4.3 ± 0.3)
Human teeth (del Pilar Gutierrez-Salazar and Reyes-Gasga, 2003)	Axial and transversal	50..60 (0.5..0.6)	270..360 (2.9..3.9)
Geological fluoroapatite single crystal	Basal faces	625 ± 17 (6.7 ± 0.2)	
	Side faces	377 ± 24 (4.1 ± 0.3)	

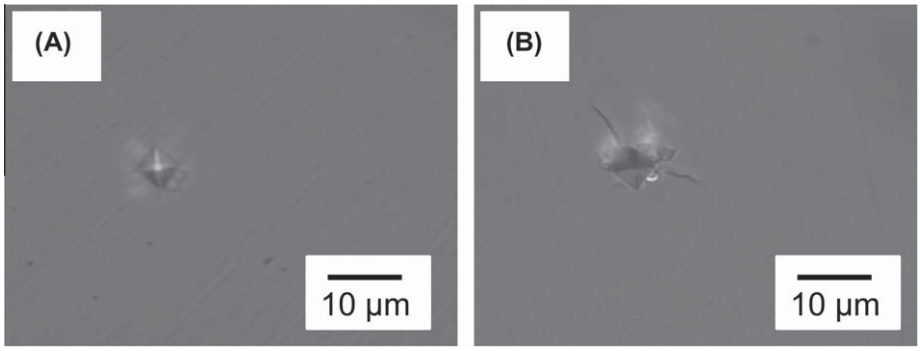

Fig.10. Representative Vicker's indentations (A) on the basal hexagonal face (indentations parallel to [0 0 1]) and (B) on the side face (indentations perpendicular to [0 0 1]) of a geological fluoroapatite crystal. Note the crack formation on the side face.

Table 3
Chemical composition of teeth of *Isurus* oxyrinchus and *Galeocerdo cuvier*, of human teeth, of a geological fluoroapatite single crystal (this work) and of stoichiometric fluoroapatite (in wt.%).

	Isurus oxyrinchus		*Galeocerdo cuvier*		Human teeth (LeGeros, 1981)		Geological fluoroapatite single crystal	Calculated for stoichiometric fluoroapatite
	Dentin	Enameloid	Dentin	Enameloid	Dentin	Enamel		
Ca^{2+}	30.90	37.81	24.26	31.19	27.0	36.0	38.42	39.74
PO_4^{3-}	48.20	54.35	41.80	51.55	39.9[a]	54.3[a]	53.25	56.50
Ca/P molar ratio	1.52:1	1.65:1	1.38:1	1.43:1	1.60:1	1.57:1	1.71:1	1.67:1
Na^+	1.14	1.03	1.35	0.99	0.3	0.5	0.18	0
Mg^{2+}	0.44	0.13	0.82	0.29	1.1	0.44	$<3 \times 10^{-6}$	0
F^-	0.61	3.08	1.46	3.13	0.05	0.01	3.64	3.77

[a] Calculated from phosphorous content.

IR spectra of the shark teeth showed the characteristic bands of biological apatite (phosphate: 490–640 cm^{-1} and 900–1360 cm^{-1}, carbonate: 875 cm^{-1} and 1360–1590 cm^{-1}, water: 3010–3660 cm^{-1}) (Fig. 12). The shape of the carbonate bands (many small bands) in the range of 1360–1590 cm^{-1} indicated a B-type substitution of carbonate in the lattice (CO_3^{2-} for PO_4^{3-} and Na^+ for Ca^{2+}). A-type substitution (CO_3^{2-} for OH^-) would lead to two sharp bands in this IR-range. B-Type substitution of carbonate occurs in aqueous environments (like seawater). In contrast, A-type substitution of carbonate occurs at high temperature and dry conditions (LeGeros, 1994). In addition to the apatite bands, a weak C–H-band (2940 cm^{-1}) and a carbonyl-band (1600–1700 cm^{-1}) were visible due to the presence of the organic matrix in the tooth samples. The bands of phosphate were better resolved in the enameloid than in dentin due to the higher crystallinity of enameloid mineral. The IR spectrum of the geological fluoroapatite single crystal confirms the above assignments.

Thermogravimetry of dentin and enameloid of both shark species showed three main regions (Fig. 13). First, the release of water (up to 200 °C), then the combustion of the organic matrix (200 to 500 °C), and finally (>500 °C) the release of CO_2 from carbonated apatite (LeGeros, 1981; Peters et al., 2000).

4. Discussion

Although the teeth of the two shark species have different biological function, i.e., tearing for *I. oxyrinchus* and cutting for *G. cuvier*, their hardness was comparable both on the micro- and on the nanoscale. This suggests that the different tooth function is not accomplished by different hardness, but merely by different form. The constituting structural elements (fluoroapatite rods in enameloid and collagen fibers in dentin) are interdigitated, giving a mechanically strong structure in all directions. As expected, enameloid was much harder than dentin in good agreement with earlier work on shark teeth (Chen et al., 2008).

The variation in nanohardness is due to the inhomogeneous distribution of the biomineral in the teeth and the small sampling area in nanoindentation. There were apatite crystals which showed a higher hardness (comparable to the results of the nanoindentation on the geological fluoroapatite single crystal) and areas with organic matrix which showed a lower hardness.

Nanoindentation data of shark teeth were reported earlier for *Sphyrna tiburo* and *Carcharias taurus* by Whitenack et al. (2010). The hardness of the enameloid ranged from 3.0–3.8 Gpa, and the reduced elastic modulus ranged from 67.4–77.3 GPa. The values of hardness and reduced elastic modulus of the enameloid of *I. oxyrinchus* and *G. cuvier* (about 6 GPa and 100 GPa, respectively) were higher than the values reported by Whitenack et al. (2010). The reason for this difference is not known, but possibly the lower load (300 µN) and thus the lower indentation depth (about 0.03–0.13 µm) compared to the 2 µm indentation depth observed by Whitenack et al. (2010) lead to strain hardening. Notably, it was reported that the values from nanoindentation compared to microindentation are about 10–30% higher in metals (Qian et al., 2005).

The tooth tip was not harder than other areas in the enameloid. This is in good agreement with Whitenack et al. (2011) who analyzed the von Mises stress of teeth of *I. oxyrinchus* and *G. cuvier*. This also justifies our use of only the tooth tip as pure enameloid for the thermogravimetric measurements. The fluoride content of the shark teeth was much higher than that of human teeth and close to stoichiometric fluoroapatite (Table 3). Similar results were obtained by Glas (1962) with 3.3 wt.% fluoride for shark teeth enameloid. In comparison, the fluoride content in the mineral in dentin was much smaller, indicating the presence of fluorohydroxyapatite (francolite), and also suggesting that the fluoride content in the enameloid serves some hitherto unknown function which is not only related to the hardness.

The presence of fluoride in the apatite lattice was confirmed by the analysis of the unit cell parameters. The length of the *c*-axis of hydroxyapatite and fluoroapatite is almost identical and therefore

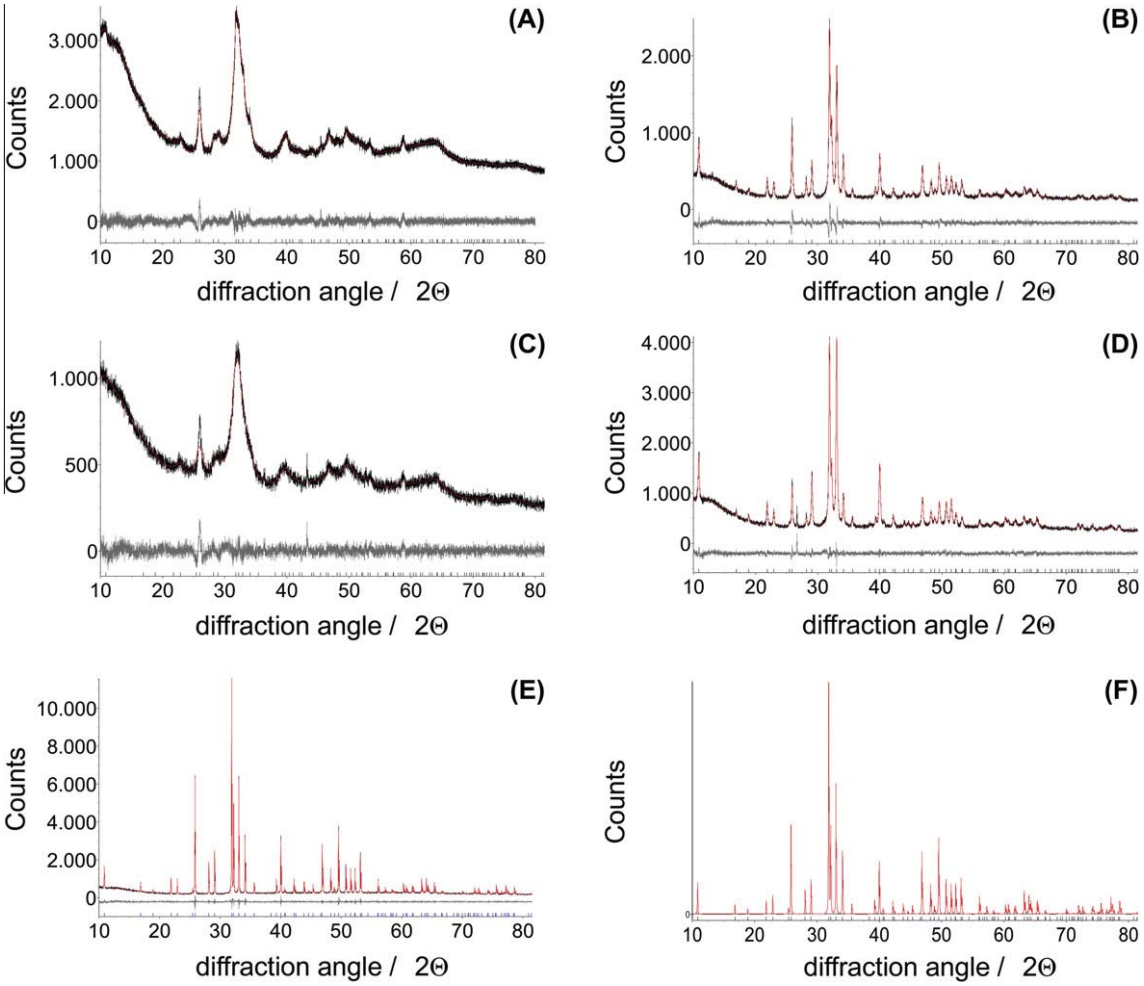

Fig.11. X-ray powder diffractograms of *Isurus oxyrinchus* dentin (A), *Isurus oxyrinchus* enameloid (B), *Galeocerdo cuvier* dentin (C), *Galeocerdo cuvier* enameloid (D), a geological fluoroapatite single crystal (E), and a calculated diffractogram of fluoroapatite (F). Black: experimental data; red: calculated Rietveld fit data.

Table 4
Crystallographic properties of dentin and enameloid of teeth of *Isurus oxyrinchus* and *Galeocerdo cuvier*, of a geological fluoroapatite single crystal and of synthetic hydroxyapatite.

Shark species		*a*-axis (Å)	*c*-axis (Å)	*V* (Å^3)
Isurus oxyrinchus	Dentin	9.403(2)	6.852(2)	524.6(3)
	Enameloid	9.38346(1)	6.88481(1)	524.99(1)
Galeocerdo cuvier	Dentin	9.405(5)	6.832(5)	523.4(7)
	Enameloid	9.3874(2)	6.8816(2)	525.18(3)
Geological fluoroapatite single crystal		9.37500(3)	6.88847(3)	524.319(4)
Synthetic hydroxyapatite		9.4471(6)	6.8848(4)	532.13(7)
Synthetic fluoroapatite (Rodriguez-Lorenzo et al., 2003)		9.3716(1)	6.8843(1)	523.62
Geological hydroxyapatite (Saenger and Kuhs, 1992)		9.4249(4)	6.8838(4)	529.56

Table 5
Crystallite sizes (domaine sizes) in nm, calculated from X-ray powder diffractograms with the Scherrer equation.

Diffraction line index	(110)	(111)	(002)	(210)	(030)	(310)	(222)	(213)	(004)
Diffraction angle (2Θ°)	18.9	22.9	25.9	29.1	33.0	40.0	46.8	49.6	53.2
Galeocerdo cuvier, enameloid	32	54	48	43	37	37	49	75	53
Isurus oxyrinchus, enameloid	34	45	42	41	37	34	44	50	52
Galeocerdo cuvier, dentin	–	11	10	2.4	–	2.2	–	–	–
Isurus oxyrinchus, dentin	–	8	13	2.0	–	2.1	–	–	–

of little value to assess the fluoride substitution. The *a*-axes of the enameloid and of the geological fluoroapatite single crystal were shorter than that of the synthetic hydroxyapatite. This underscores the earlier results by LeGeros and Suga (1980) on fluoroapatite: they reported that the substitution of hydroxyde by fluoride leads to a shorter *a*-axis with an unaffected *c*-axis length. Using the

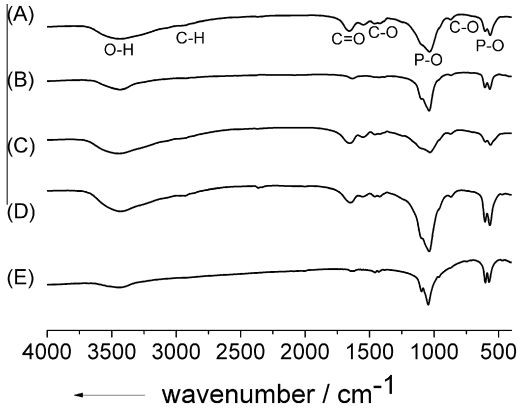

Fig.12. IR transmission spectra of *Isurus oxyrinchus* dentin (A), *Isurus oxyrinchus* enameloid (B), *Galeocerdo cuvier* dentin (C), *Galeocerdo cuvier* enameloid (D), and a geological fluoroapatite single crystal (E).

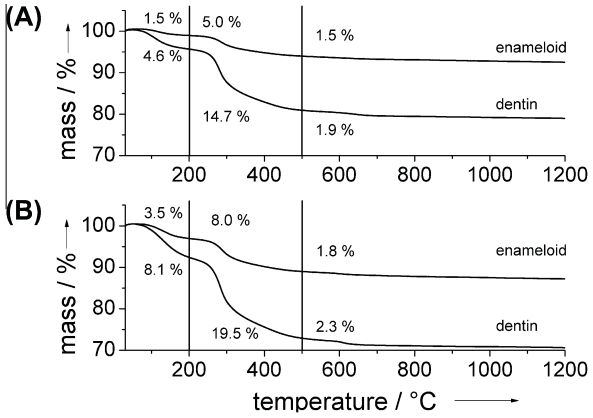

Fig.13. Thermogravimetry of teeth of *Isurus oxyrinchus* (A) and *Galeocerdo cuvier* (B): <200 °C: release of water, 200–500 °C: combustion of the organic matrix, and >500 °C: release of CO_2 from carbonated apatite.

correlative graph from LeGeros and Suga (1980) with a linear relationship between the length of the *a*-axis and the fluoride concentration, we estimated a content of about 3.4 wt.% fluoride for the enameloid of both shark species, in good agreement with the elemental analysis results. The contents of sodium and magnesium were higher in dentin than in enameloid.

The dentin had a higher content of water than the enameloid, and the enameloid in turn had a lower content of organic matrix and carbonate. The comparatively high contents of organic matrix in the shark teeth enameloid (*I. oxyrinchus*: 5 wt.% and *G. cuvier*: 8 wt.%) in comparison to human teeth are probably due to the presence of some residual dentin because at least 20 mg were necessary for thermogravimetry. The other values were comparable to human teeth according to LeGeros (1981): adsorbed water (dentin 10.6 wt.%; enamel 1.5 wt.%), organic matrix (dentin 20.0 wt.%; enamel 1.0 wt.%) and carbonate (dentin 4.5 wt.%; enamel 2.3 wt.%). Note that the content of adsorbed water varies is variable due to different preparation and storage of the teeth.

In contrast to dentin, enameloid of both shark species showed sharp diffraction peaks of apatite in the X-ray powder diffractograms, indicating a high crystallinity. In dentin, broad diffraction peaks indicated a nanocrystalline biomineral (Fig. 11).

Nano- and microhardness were comparable for shark teeth and for human teeth, both for dentin and enamel. This means that the hardness of the teeth is independent from the kind of apatite (human teeth: hydroxyapatite; shark teeth: fluoroapatite). The incorporation of fluoride into the apatite lattice had no significant effect on the micro- and nanohardness of the teeth.

The content of calcium phosphate in the enameloid of both shark species was higher than in the dentin, showing the higher mineral content in enameloid, in agreement with the results reported by Suga et al. (1982) for 78 perciform fish species, comprising marine fish, primary and secondary freshwater fish, and vicarious freshwater fish.

The higher mechanical strength of enameloid in comparison to dentin from nanoindentation and Vicker's hardness test is due to the higher mineral content of enameloid (elemental analysis and TG) and higher crystallinity (SEM, XRD, and IR). A dependence of the nanohardness on the calcium content and thus the mineral content, was also found in human teeth. If the calcium content decreases, the nanohardness decreases as well (Cuy et al., 2002; Jeng et al., 2011). Similar results were found for compact bones of mammals, birds, and reptiles (Currey, 1988).

The fact that the mineral produced a higher mechanical strength than the organic matrix was confirmed by the analysis of the hardness of geological fluoroapatite single crystals. The geological fluoroapatite single crystal was significantly harder than the teeth (which additionally contained an organic matrix). In our nanoindentation tests, no significant anisotropy was found between basal and side faces. Saber-Samandari and Gross (2009) and Viswanath et al. (2007) found a small anisotropy by nanoindentation on hydroxyapatite single crystals and hardness values comparable to our results. In contrast, we found a difference in both directions by Vicker's hardness tests. This can be explained by examining the crack formation on the single crystal faces. The cracks that formed on a side face were larger than those on a hexagonal basal face. Crack formation was also observed during microindentation by Viswanath et al. (2007) on a hydroxyapatite single crystal. In Vicker's hardness tests, the crack formation is of higher importance compared to nanoindentation because of the 0.1 N load. In contrast, in nanoindentation tests, only 300 μN are applied and, thus, crack formation plays a negligible role. Sha et al. (1994) have found no strong anisotropy in the elastic constants of a fluoroapatite single crystal by measuring the ultrasound velocity. Teraoka et al. (1998) have determined the elastic modulus of hydroxyapatite single crystals by three-point bending to 54–79 GPa. Brunet et al. (1999) obtained isothermal bulk moduli of 97.5 ± 1.8 GPa for hydroxyapatite and 97.9 ± 1.9 GPa for fluoroapatite by in situ X-ray diffraction during compression. Matsukage et al. (2004) obtained an isothermal bulk modulus of 91.5 ± 3.8 GPa for a fluoroapatite single crystal by the same method. This in summary confirms our results.

5. Conclusions

Both studied shark teeth have a comparable chemical and crystallographic composition. Enameloid has a much higher mineral content than dentin, and also contains larger crystals. The crystals in enameloid consist of bundles with a special arrangement. The biomineral is a carbonated apatite with almost stoichiometric fluoride content in enameloid but with much smaller fluoride content in dentin. Nanoindentation (nanohardness) and Vicker's hardness tests (microhardness) showed that the enameloid of both shark teeth was approximately six times harder than the dentin with an isotropic hardness that was independent of the direction of the cut or the indentation. Although fluoroapatite has a higher hardness compared to hydroxyapatite, the shark teeth enameloid (fluoroapatite) was not harder than the enamel of human teeth (hydroxyapatite). A geological single crystal of fluoroapatite was much harder but also more brittle due to the absence of an organic matrix. Thus, the shark teeth represent a highly optimized

structure for the different biological purposes like cutting and ripping, but their chemical composition the crystallographic nature of the biomineral is very similar for both species. The fact that sharks use fluoroapatite as tooth biomineral instead of hydroxyapatite which is used by mammals does not lead by a higher hardness of the shark teeth and must have a different, but hitherto unknown, reason.

Acknowledgments

We thank the following members of the Max-Planck-Institut für Eisenforschung, Düsseldorf, Germany for their support: Dr. H. Fabritius, K. Angenendt and M. Nellessen for the SEM–BSE-measurements, H. Bögershausen for the nanoindentation, and H. Faul for the Vicker's hardness tests. We thank Dr. A. Gillis, Department of Physiology, Development and Neuroscience, University of Cambridge, for help with the taxonomic determination of the shark species. We thank C. Fischer, Essen, for help with the tooth preparation.

References

Absi, E.G., Addy, M., Adams, D., 1987. Dentine hypersensitivity. A study of the patency of dentinal tubules in sensitive and non-sensitive cervical dentine. J. Clin. Periodontol. 14, 280–284.

Al-Sawalmih, A., Li, C.H., Siegel, S., Fabritius, H., Yi, S.B., et al., 2008. Microtexture and chitin/calcite orientation relationship in the mineralized exoskeleton of the American lobster. Adv. Funct. Mater 18, 3307–3314.

Brunet, F., Allan, D.R., Redfern, S.A.T., Angel, R.J., Miletich, R., et al., 1999. Compressibility and thermal expansivity of synthetic apatites, $Ca_5(PO_4)_3X$ with X = OH, F and Cl. Eur. J. Mineral. 11, 1023–1035.

Chen, P.Y., Lin, A.Y.M., Lin, Y.S., Seki, Y., Stokes, A.G., et al., 2008. Structure and mechanical properties of selected biological materials. J. Mech. Behav. Biomed. Mater. 1, 208–226.

Currey, J.D., 1988. The effect of porosity and mineral content on the Young's modulus of elasticity of compact bone. J. Biomech. 21, 131–139.

Cuy, J.L., Mann, A.B., Livi, K.J., Teaford, M.F., Weihs, T.P., 2002. Nanoindentation mapping of the mechanical properties of human molar tooth enamel. Arch. Oral. Biol. 47, 281–291.

Daculsi, G., Kerebel, L.M., 1980. Ultrastructural study and comparative analysis of fluoride content of enameloid in sea-water and fresh-water sharks. Arch. Oral Biol. 25, 145–151.

Dahm, S., Risnes, S., 1999. A comparative infrared spectroscopic study of hydroxide and carbonate absorption bands in spectra of shark enameloid, shark dentin, and a geological apatite. Calcif. Tissue Int. 65, 459–465.

Del Pilar Gutierrez-Salazar, M., Reyes-Gasga, J., 2003. Microhardness and chemical composition of human tooth. Mater. Res. 6, 367–373.

Dorozhkin, S.V., Epple, M., 2002. Biological and medical significance of calcium phosphates. Angew. Chem. Int. Ed. 41, 3130–3146.

Dunlop, J.W.C., Fratzl, P., 2010. Biological composites. In: Clarke, D.R. et al. (Eds.), Annual Review of Materials Research, vol. 40. Annual Reviews, Palo Alto, pp. 1–24.

Dyson, N.A., 2005. X-rays in Atomic and Nuclear Physics. Cambridge University Press, Cambridge.

Fabritius, H., Sachs, C., Triguero, P., Raabe, D., 2009. Influence of structural principles on the mechanics of a biological fiber-based composite material with hierarchical organization: the exoskeleton of the lobster *Homarus americanus*. Adv. Mater. 21, 391–400.

Fincham, A.G., Moradian-Oldak, J., Simmer, J.P., 1999. The structural biology of the developing dental enamel matrix. J. Struct. Biol. 126, 270–299.

Frazzetta, T.H., 1988. The mechanics of cutting and the form of shark teeth (Chondrichthyes, Elasmobranchii). Zoomorphology 108, 93–107.

Gardner, T.N., Elliott, J.C., Sklar, Z., Briggs, G.A., 1992. Acoustic microscope study of the elastic properties of fluorapatite and hydroxyapatite, tooth enamel and bone. J. Biomech. 25, 1265–1277.

Gillis, J.A., Donoghue, P.C.J., 2007. The homology and phylogeny of chondrichthyan tooth enameloid. J. Morphol. 268, 33–49.

Glas, J.E., 1962. The ultrastructure of dental enamel. VI. Crystal chemistry of shark's teeth. Odontol. Rev. 13, 315–326.

Herold, R.C., Graver, H.T., Christner, P., 1980. Immunohistochemical localization of amelogenins in enameloid of lower vertebrate teeth. Science 207, 1357–1358.

Jeng, Y.R., Lin, T.T., Hsu, H.M., Chang, H.J., Shieh, D.B., 2011. Human enamel rod presents anisotropic nanotribological properties. J. Mech. Behav. Biomed. Mater. 4, 515–522.

Kemp, N.E., 1984. Organic matrices and mineral crystallites in vertebrate scales, teeth and skeletons. Am. Zool. 24, 965–976.

Kesmez, M., Lyon, J., Cocke, D.L., Westgate, J., McWhinney, H., et al., 2004. Characterization of the evolutionary aspects of great white shark teeth by x-ray diffraction methods and other supporting techniques. Adv. X-Ray Anal. 47, 327–337.

Klug, H.P., Alexander, L.E., 1974. X-ray Diffraction Procedures for Polycrystalline and Amorphous Materials. Wiley-Interscience, New York.

Kovtun, A., Kozlova, D., Ganesan, K., Biewald, C., Seipold, N., et al., 2012. Chlorhexidine-loaded calcium phosphate nanoparticles for dental maintenance treatment: combination of mineralising and antibacterial effects. RSC Adv. 2, 870–875.

LeGeros, R.Z., 1981. Apatites in biological systems. Prog. Cryst. Growth Charact. 4, 1–45.

LeGeros, R.Z., 1990. Chemical and crystallographic events in the caries process. J. Dent. Res. 69, 567–574, 634–636.

LeGeros, R.Z., 1994. Biological and synthetic apatites. In: Brown, P.W., Constantz, B. (Eds.), Hydroxyapatite and Related Materials. CRC Press, Boca Raton, pp. 3–28.

LeGeros, R.Z., Suga, S., 1980. Crystallographic nature of fluoride in enameloids of fish. Calcif. Tissue Int. 32, 169–174.

Lowenstam, H.A., Weiner, S., 1989. On Biomineralization. Oxford University Press, New York.

Mann, S., 2001. Biomineralization. Oxford University Press, Oxford.

Marshall, G.W., Habelitz, S., Gallagher, R., Balooch, M., Balooch, G., et al., 2001. Nanomechanical properties of hydrated carious human dentin. J. Dent. Res. 80, 1768–1771.

Marten, A., Fratzl, P., Paris, O., Zaslansky, P., 2010. On the mineral in collagen of human crown dentine. Biomaterials 31, 5479–5490.

Matsukage, K.N., Ono, S., Kawamoto, T., Kikegawa, T., 2004. The compressibility of a natural apatite. Phys. Chem. Miner. 31, 580–584.

Moeller, I.J., Melsen, B., Jensen, S.J., Kirkegaard, E., 1975. A histological, chemical, and X-ray diffraction study on contemporary (*Carcharias glaucus*) and fossilized (*Macrota odontaspis*) shark teeth. Arch. Oral Biol. 20, 797–802.

Oliver, W.C., Pharr, G.M., 1992. An improved technique for determining hardness and elastic modulus using load and displacement sensing indentation experiments. J. Mater. Res. 7, 1564–1583.

Peters, F., Schwarz, K., Epple, M., 2000. The structure of bone studied with synchrotron X-ray diffraction, X-ray absorption spectroscopy and thermal analysis. Thermochim. Acta 361, 131–138.

Powlik, J.J., 1995. On the geometry and mechanics of tooth position in the white shark, *Carcharodon carcharias*. J. Morphol. 226, 277–288.

Preuschoft, H., Reif, W.E., Müller, W.H., 1974. Funktionsanpassungen in Form und Struktur an Haifischzähnen. Anat. Embryol. 143, 315–344.

Qian, L., Li, M., Zhou, Z., Yang, H., Shi, X., 2005. Comparison of nano-indentation hardness to microhardness. Surf. Coat. Technol. 195, 264–271.

Reif, W.E., 1974. Morphologie und Ultrastruktur des Hai-"Schmelzes". Zool. Scr. 2, 231–250.

Rodriguez-Lorenzo, L.M., Hart, J.N., Gross, K.A., 2003. Structural and chemical analysis of well-crystallized hydroxyfluorapatites. J. Phys. Chem. B 107, 8316–8320.

Saber-Samandari, S., Gross, K.A., 2009. Micromechanical properties of single crystal hydroxyapatite by nanoindentation. Acta Biomater. 5, 2206–2212.

Sachs, C., Fabritius, H., Raabe, D., 2006. Hardness and elastic properties of dehydrated cuticle from the lobster *Homarus americanus* obtained by nanoindentation. J. Mater. Res. 21, 1987–1995.

Saenger, A.T., Kuhs, W.F., 1992. Structural disorder in hydroxyapatite. Z. Kristallogr. 199, 123–148.

Sha, M.C., Li, Z., Bradt, R.C., 1994. Single-crystal elastic-constants of fluorapatite, $Ca_5F(PO_4)_3$. J. Appl. Phys. 75, 7784–7787.

Stock, S.R., Vieira, A.E.M., Delbem, A.C.B., Cannon, M.L., Xiao, X., et al., 2008. Synchrotron microcomputed tomography of the mature bovine dentinoenamel junction. J. Struct. Biol. 161, 162–171.

Suga, S., Taki, Y., Wada, K., 1982. Fluoride concentration in the teeth of perciform fishes and its phylogenetic significance. Jap. J. Ichthyol. 30, 81–93.

Teaford, M.F., Smith, M.M., Ferguson, M.W.J., 2000. Development, Function and Evolution of Teeth. Cambridge University Press, Cambridge.

Teraoka, K., Ito, A., Maekawa, K., Onuma, K., Tateishi, T., et al., 1998. Mechanical properties of hydroxyapatite and OH-carbonated hydroxyapatite single crystals. J. Dent. Res. 77, 1560–1568.

Viswanath, B., Raghavan, R., Ramamurty, U., Ravishankar, N., 2007. Mechanical properties and anisotropy in hydroxyapatite single crystals. Scr. Mater. 57, 361–364.

Wang, R., Weiner, S., 1998a. Human root dentin: structural anisotropy and Vickers microhardness isotropy. Conn. Tissue Res. 39, 269–279.

Wang, R.Z., Weiner, S., 1998b. Strain–structure relations in human teeth using Moiré fringes. J. Biomechan. 31, 135–141.

Weiner, S., Addadi, L., 1997. Design strategies in mineralized biological materials. J. Mater. Chem. 7, 689–702.

Whitenack, L.B., Motta, P.J., 2010. Performance of shark teeth during puncture and draw: implications for the mechanics of cutting. Biol. J. Linn. Soc. 100, 271–286.

Whitenack, L.B., Simkins Jr., D.C., Motta, P.J., 2011. Biology meets engineering: the structural mechanics of fossil and extant shark teeth. J. Morphol. 272, 169–179.

Whitenack, L.B., Simkins Jr., D.C., Motta, P.J., Hirai, M., Kumar, A., 2010. Young's modulus and hardness of shark tooth biomaterials. Arch. Oral Biol. 55, 203–209.

Willems, G., Celis, J.P., Lambrechts, P., Braem, M., Vanherle, G., 1993. Hardness and Young's modulus determined by nanoindentation technique of filler particles of dental restorative materials compared with human enamel. J. Biomed. Mater. Res. 27, 747–755.

Zabler, S., Cloetens, P., Zaslansky, P., 2007. Fresnel-propagated submicrometer X-ray imaging of water-immersed tooth dentin. Optics Lett. 32, 2987–2989.